

Optimal Partitioning of Smart Distribution Systems into Supply-Sufficient Microgrids

Mostafa Barani, *Student Member, IEEE*, Jamshid Aghaei, *Senior Member, IEEE*, Mohammad Amin Akbari, Taher Niknam, *Member, IEEE*, Hossein Farahmand, *Member, IEEE*, and Magnus Korpås, *Member, IEEE*,

Abstract—This paper presents a systematic procedure for partitioning smart distribution systems into supply-sufficient microgrids. Firstly, renewable distributed generations (DGs) are optimally allocated in the distribution system. A multiobjective performance index including voltage profile and energy losses indices is utilized in this problem as the objective function. Two alternative control approaches of future smart grids including on load tap changer (OLTC) control and adaptive power factor control (PFC) are assessed to maximize potential benefits and increase the penetration level of DGs. Then, optimal allocation of protection devices and energy storage systems (ESSs) for constructing supply-sufficient microgrids is presented for a feeder equipped with capacity-constrained DGs. To this end, two different optimization problems are formulated and proper indices are developed for minimizing power exchange between microgrids and minimizing generation-load imbalance within microgrids. Finally, test results of the proposed models on 33-bus IEEE radial distribution system are presented and discussed.

Index Terms—Distributed generation, microgrid, supply adequacy, smart grid, wind energy, energy storage systems.

I. INTRODUCTION

INCREASING reliance on variable renewable energy sources is driving changes in the conventional planning and operation of distribution systems [1]–[3]. To mitigate the impacts of the interconnection of renewable generation, the concepts of smart grids are proposed widely. According to the IEEE Std 1547.4, large distribution systems can be partitioned into a number of microgrids to facilitate powerful control and operation infrastructure in the future distribution systems [4]. In this regard, increasing controllability and flexibility of the (variable) supply and demand is a key pathway toward a more robust systems [5].

Microgrids have been proposed as a novel distribution network architecture within the smart grids concept which is capable to exploit the full benefits from the integration of large numbers of small scale distributed energy resources (DERs) into low-voltage electricity distribution systems [6]–[8]. A microgrid can be operated in an islanded mode, in the event of an upstream fault, and a grid-connected mode. To be able to operate in the island mode, DERs, i.e., both DGs and energy storage systems (ESSs), have to be able to serve the island load and therefore keep both the voltage and frequency within allowable limits. Hence, they can

reduce the impacts of faults on their local loads by creating islands of supply to increase the reliability of service. Therefore, adequacy of supply for microgrids is an important factor in the optimal microgrid construction (OMGC) which enhances the distribution system to be a self-heal and robust system [7], [8].

DERs play an important role in the construction of microgrids. The effects of these resources on the distribution system and microgrids were examined in [3], [6]–[21]. The allocation of DG units in distribution systems has been investigated in the literature from different perspectives which primarily takes the technical and economic issues into account. The large number of works have focused on computational methods and approaches employed in the optimal DG allocation (ODGA) problem [3], [6]–[11]. They have attempted to find optimal DGs sites and sizes to be set up for use in the distribution networks with the objectives of minimizing total costs, losses minimization, voltage stability and installed capacity maximization subject to the technical, DGs operation, and investment constraints. The benefits and risks issues of introducing DGs in the distribution systems have been explored in [12]–[15]. One of the major challenges for DGs that is still remained in matching the intermittent energy production with the dynamic power demand. A recommended solution is to add ESSs into the intermittent output power of DGs such as wind turbines and photovoltaic (PV) modules. Cost and reliability effects of DGs and ESS have been investigated in [15]–[17]. Numerous works have been done to assess the reliability and economy of small autonomous power systems and microgrids using both analytical and Monte Carlo simulation (MCS) methods, when renewable DGs are operated in either islanded or grid-connected modes [7], [8], [16]–[21].

Overall, few studies properly investigate the adequacy-based OMGC in distribution systems considering probabilistic nature of renewable generation and demand. Additionally, the potential advantages of adopting real-time control and communication systems, as the main parts of the future smart grids, for the optimal allocation of DGs, ESSs and protective devices have been largely ignored.

Based on IEEE Std 1547.4, the microgrids have been introduced as the main components of active distribution networks. However, the objectives of their construction have not been determined in this standard. This paper proposes an adequacy-based OMGC problem consistent with the mentioned standard and enhances it by developing a systematic strategy for OMGC in the smart grids. The goal of design is the construction of supply-sufficient microgrids by optimally implementing dispatchable and renewable DGs (considering their intermittency and uncertainty), ESSs as well as protective devices. The motivations toward the proposed partitioning technique can be summarized as follows:

- To assist utility engineers and system planners in constructing supply-sufficient microgrids which can be a helpful step toward

M. Barani, M. Akbari, and T. Niknam are with the Department of Electrical and Electronics Engineering, Shiraz University of Technology, Shiraz, Iran (e-mail: m.barani@sutech.ac.ir; m.akbari@sutech.ac.ir; niknam@sutech.ac.ir).

J. Aghaei is with the Department of Electrical and Electronics Engineering, Shiraz University of Technology, Shiraz, Iran and the Department of Electric Power Engineering, Norwegian University of Science and Technology (NTNU), Trondheim, Norway (e-mail: aghaei@sutech.ac.ir).

Hossein Farahmand and Magnus Korpås are with the Department of Electric Power Engineering, Norwegian University of Science and Technology (NTNU), Trondheim, Norway (e-mail: hossein.farahmand@ntnu.no; magnus.korpas@ntnu.no).

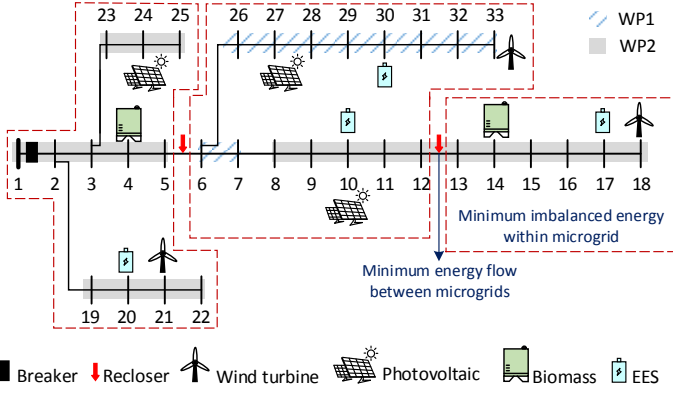


Fig. 1. Conceptual design of RDS partitioning into a set of supply-sufficient microgrids by strategically placement of DGs, ESS and reclosers; the corresponding reliability zones (microgrids) defined by dashed lines.

the realization of more secure and robust smart distribution grids.

- To advance the progress of making powerful infrastructure for smart distribution systems operation and control, like self-healing control by improving, for example, the effectiveness of the automatic fault location detection methods employed in the distribution networks.
- Since each microgrid is constructed with the maximum supply adequacy, it can improve the capability of self-healing control actions by minimizing number of actions needed in the distribution systems.
- In face of disturbances, a self-healing reconfiguration divides the system into partitions that are designed to have minimum interaction and therefore any disturbances in a particular partition will not strongly propagate to the other partitions. This can increase the performance and robustness of the distribution networks, as well as minimize total amount of load shedding in the islanded microgrids.

Accordingly, the main contributions of this work with respect to the previous researches in the area are summarized as follows:

- 1) A two-step computational framework is developed for optimal partitioning of smart distribution system. The first step determines optimal placement of renewable DGs to maximize multiobjective performance index. In the second step, protective devices and ESSs are simultaneously placed and sized for construction of supply-sufficient microgrids to improve self-healing control mechanisms in the smart distribution systems.
- 2) Proper adequacy-based metrics are introduced for evaluation of the supply-adequacy of the constructed microgrids within distribution systems.
- 3) Linear formulations are developed for the OMGC problem. As a result, the problem can be solved using mixed-integer linear programming (MILP) through one of the high-performance commercially available solvers like CPLEX and OSL.

The rest of the paper is organized as follows: Section II describes the modeling of the renewable DGs, load, network and generation-load. The problem formulation of ODGA is addressed in Section III. OMGC problem is introduced in Section IV. The results obtained by applying the proposed models to a variety of case studies are demonstrated in Section V. Finally, the conclusions are summarized in Section VI.

II. MODEL DESCRIPTION

In this paper, the period of the study is one year. This year is divided into four seasons and each season is modeled through a typical day with 24-hour time period. Therefore, the year under study can be modeled with 96-hour time period.

A. Probabilistic Modeling of DGs

The hourly historical data related to the wind speed and solar irradiance during two whole years has been utilized to model probabilistic generation of each DG unit. In order to characterize the random behavior of the renewable energy resources during each season, a typical day with 24-hour time period is considered. For each season, the data related to the same hours of the days in the related season are utilized to obtain the hourly probability density functions (PDFs). Since two years of historical data are available and by assuming a month to be 30 days, there are 180 samples (2 years \times 3 months \times 30 days) of wind speed and solar irradiance to generate the related hourly PDFs. Therefore, there are 180 samples to estimate each of the 96 PDFs related to each hourly time period.

In this study, the hourly wind speed and solar irradiance have been utilized to generate Rayleigh [3] and Beta [22] distribution functions for each time period as indicated in (1) and (2), respectively.

$$f_b(s) = \begin{cases} \frac{\Gamma(\alpha + \beta)}{\Gamma(\alpha) \cdot \Gamma(\beta)} s^{(\alpha-1)} (1-s)^{(\beta-1)} & : 0 \leq s \leq 1; \alpha, \beta \geq 0 \\ 0 & : \text{otherwise.} \end{cases} \quad (1)$$

where $f_b(\cdot)$ denotes the Beta distribution function. α and β are the parameters of the Beta function and for each time period, can be determined using the historical data.

$$f_r(v) = \left(\frac{2v}{c^2}\right) \exp\left[-\left(\frac{v}{c}\right)^2\right] \quad (2)$$

where $f_r(\cdot)$ indicates Rayleigh distribution function and c is Rayleigh scale index which is determined based on the historical data for each time period.

These continuous PDFs are sliced into several segments where each segment yields a mean value and a probability of occurrence. Note that the probability of each segment during any specific hour can be expressed as follows:

$$\text{prob}_i = \int_{X_i}^{X_{i+1}} f(x) dx \quad (3)$$

where $f(x)$ indicates PDFs. X_i and X_{i+1} are the starting and ending points of the interval i , respectively.

It should be noted that for the site under study two different wind profiles, i.e., WP1 and WP2, are considered in this paper. Algorithm 1 indicates the process of scenario generation for uncertain parameters. The uncertainties of the problem, i.e., wind speed of WP1, wind speed of WP2, and solar irradiance,

Algorithm 1 Probabilistic Model of Whole System.

Require: Historical data and parameters as follows:

- Data related to *wind-based DG* (historical data of hourly wind speed for WP1 and WP2, wind turbine performance curve).
- Data related to *solar DG* (Historical data of solar irradiance, PV module characteristics).
- Number of scenarios in the initial scenario sets for the wind speed of WP1 (N_{wp1}), the wind speed of WP2 (N_{wp2}), and solar irradiance N_s and the reduced sets (N_{wp1}^r , N_{wp2}^r , N_s^r).

1: Construct the hourly PDFs related to *i*) solar irradiance, *ii*) wind speed of WP1, *iii*) wind speed of WP1.

2: Utilize the procedure discussed in [23] to generate the scenarios using the PDFs:

- N_{wp1} scenarios for the wind speed of WP1;
- N_{wp2} scenarios for the wind speed of WP2;
- N_s scenarios for the solar irradiance;

For instance, we use 96 hourly PDFs of wind speed of WP1 and generate N_s scenarios with their own probability. Note that each scenario include 4×24 values of hourly solar irradiance represents a year and its probability of occurrence.

3: Based on the wind turbine performance curve and PV module characteristics, the wind speed and solar irradiance of each state during each time period is transformed into the output power of wind-based and solar DGs, respectively.

4: A fast forward scenario reduction method based on Kontorwish distance [24] is employed to reduce the number of scenarios while provides a reasonable approximation of random variable of the system.

are characterized by generating N_{wp1}^r , N_{wp2}^r and N_s^r scenarios, respectively. N_{wp1}^r scenarios can represent WP1 where each scenario will include 96 generation values with its corresponding probability. Therefore, the $s1$ th scenario of WP1 with a probability ρ_{wp1}^{s1} is $\{(P_{wp1}^{s1}(1,1), P_{wp1}^{s1}(1,2), \dots, P_{wp1}^{s1}(t,h)), \rho_{wp1}^{s1}\}$. In a similar approach, WP2 and PV can be modeled as N_{wp2}^r and N_{pv}^r scenarios, respectively, i.e., $\{(P_{wp2}^{s2}(1,1), P_{wp2}^{s2}(1,2), \dots, P_{wp2}^{s2}(t,h)), \rho_{wp2}^{s2}\} : \forall s2$ and $\{(P_{pv}^{s3}(1,1), P_{pv}^{s3}(1,2), \dots, P_{pv}^{s3}(t,h)), \rho_{pv}^{s3}\} : \forall s3$. Considering the whole system, the total number of probable scenarios is $(N_{wp1}^r \times N_{wp2}^r \times N_{pv}^r)$. Each probable scenario $\{(s1, s2, s3) \in (N_{wp1}^r \times N_{wp2}^r \times N_{pv}^r)\}$ has a probability of $\rho_{wp1}^{s1} \times \rho_{wp2}^{s2} \times \rho_{pv}^{s3}$. By way of illustration, suppose that there are one wind and solar irradiance profile and there are two probable scenarios for each one as indicated in Fig. 2. Then, the entire system will include four (2×2) scenarios as follows:

for $s = 1$:

$$\{(P_{wp}^1(1,1), \dots, P_{wp}^1(4,24)), (P_{pv}^1(1,1), \dots, P_{pv}^1(4,24)), \rho_{wp}^1 \times \rho_{pv}^1\};$$

for $s = 2$:

$$\{(P_{wp}^2(1,1), \dots, P_{wp}^2(4,24)), (P_{pv}^2(1,1), \dots, P_{pv}^2(4,24)), \rho_{wp}^2 \times \rho_{pv}^2\};$$

for $s = 3$:

$$\{(P_{wp}^3(1,1), \dots, P_{wp}^3(4,24)), (P_{pv}^3(1,1), \dots, P_{pv}^3(4,24)), \rho_{wp}^3 \times \rho_{pv}^3\};$$

for $s = 4$:

$$\{(P_{wp}^4(1,1), \dots, P_{wp}^4(4,24)), (P_{pv}^4(1,1), \dots, P_{pv}^4(4,24)), \rho_{wp}^4 \times \rho_{pv}^4\}.$$

B. Load Data

From the hourly load data for the system under study and the IEEE-RTS system [25], the load profile is considered as a percentage of the annual peak load. Fig. 3 indicates the typical seasonal pattern of demand as a percentage of the annual peak load.

III. DistFlow EQUATIONS

A radial distribution system (RDS) can be represented by the graph $G = (\mathcal{N}, \mathcal{E})$ and the set of generator buses $\mathcal{G} \subseteq \mathcal{N}$. Let $\mathcal{N} := \{1, \dots, n\}$ denote the collection of all nodes. Each line connects an ordered pair (i, j) of nodes where node i is the

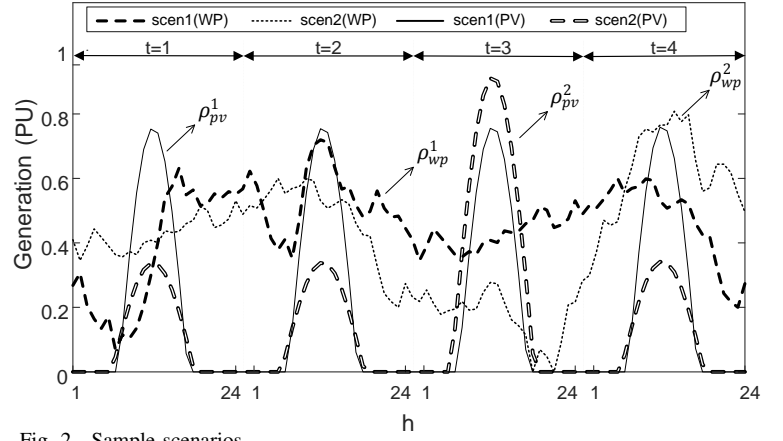


Fig. 2. Sample scenarios.

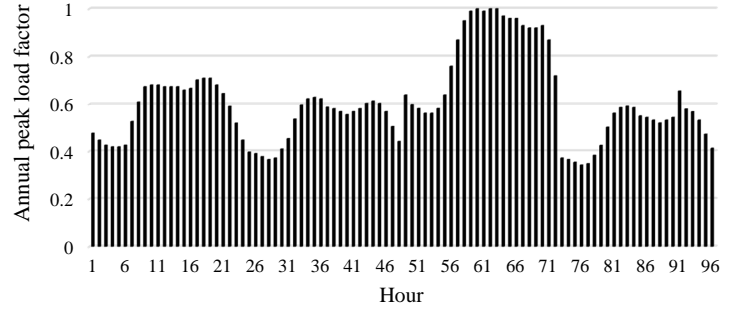


Fig. 3. Typical seasonal pattern of demand as a percentage of the annual peak load.

sending end and node j is the receiving end bus. Let \mathcal{E} denote the collection of all lines, and $(i, j) \in \mathcal{E}$ is abbreviated by $i \rightarrow j$ for convenience. Note that, as G is directed, if $(i, j) \in \mathcal{E}$ then, $(j, i) \notin \mathcal{E}$. Let t denote the index of time period ($t \in \mathcal{T}$), h indicate the index of hour ($h \in \mathcal{H}$) and s denote the index of generation-load states, where, $s \in \mathcal{S}$. For each bus $i \in \mathcal{N}$, let $V_i^s(t, h) = V_{re,i}^s(t, h) + \mathbf{i}V_{im,i}^s(t, h)$ denote its complex voltage and it is defined that $v_i^s(t, h) := |V_i^s(t, h)|^2$. Specifically, v_{sub} is the rated secondary voltage magnitude of the substation transformer, tp is the position of the OLTC and α is the change ratio per step. Let $S_{D,i}^s(t, h) = P_{D,i}^s(t, h) + \mathbf{i}Q_{D,i}^s(t, h)$ define the given apparent power of the load connected to bus $i \in \mathcal{N}$ (zero whenever bus i is not connected to any load) and $S_{DG,i}^s(t, h) = P_{DG,i}^s(t, h) + \mathbf{i}Q_{DG,i}^s(t, h)$ define the apparent power of the DG generator connected to bus $i \in \mathcal{G}$. Let $s_i^s(t, h) = p_i^s(t, h) + \mathbf{i}q_i^s(t, h)$ denote the net power injection of bus i ($S_{DG,i}^s(t, h) - S_{D,i}^s(t, h)$) where $p_i^s(t, h)$ and $q_i^s(t, h)$ denote the real and reactive power injections of bus i . For each line $(i, j) \in \mathcal{E}$, let $z_{ij} = r_{ij} + \mathbf{i}x_{ij}$ denotes its impedance. Let $I_{ij}^s(t, h) = I_{re,ij}^s(t, h) + \mathbf{i}I_{im,ij}^s(t, h)$ denotes the complex current from bus i to bus j and it is defined that $l_{ij}^s(t, h) := |I_{ij}^s(t, h)|^2$. Let $S_{ij}^s(t, h) = P_{ij}^s(t, h) + \mathbf{i}Q_{ij}^s(t, h)$ denote the sending-end power flow from bus i to bus j where $P_{ij}^s(t, h)$ and $Q_{ij}^s(t, h)$ denote the real and reactive power flow, respectively. Given the network graph $(\mathcal{N}, \mathcal{E})$, the impedance z , and the substation voltage v_{sub} , then the other decision variables satisfy the *DistFlow* equations [11]:

$$\forall (i, j) \in \mathcal{E}, \forall j \in \mathcal{N}, \forall s \in \mathcal{S}, \forall t \in \mathcal{T} \text{ and } \forall h \in \mathcal{H},$$

$$P_{ij}^s(t, h) - r_{ij}l_{ij}^s(t, h) = -p_j^s(t, h) + \sum_{k:j \rightarrow k} P_{jk}^s(t, h) \quad (4)$$

$$Q_{ij}^s(t, h) - x_{ij}l_{ij}^s(t, h) = -q_j^s(t, h) + \sum_{k:j \rightarrow k} Q_{jk}^s(t, h) \quad (5)$$

$$v_i^s(t, h) - v_j^s(t, h) = 2 [r_{ij}P_{ij}^s(t, h) + x_{ij}Q_{ij}^s(t, h)] - |z_{ij}|^2 l_{ij}^s(t, h) \quad (6)$$

$$l_{ij}^s(t, h) = \frac{P_{ij}^s(t, h)^2 + Q_{ij}^s(t, h)^2}{v_i^s(t, h)}, \quad \forall (i, j) \in \mathcal{E} \quad (7)$$

$$v_1^s(t, h) = v_{\text{sub}} + \alpha \cdot tp(t, h). \quad (8)$$

IV. ODGA IN RDS

In this section, ODGA problem is described and formulated, and the technical limits on the total DG capacity are introduced.

A. Objective Function

From the literature, two general indices have been used as the objective function of ODGA problem in distribution systems. By comparing and taking the ratio of a measure of an attribute with and without DG (with the same load pattern), an index can be derived for loss reduction and voltage profile improvement. The snapshot indices have been proposed in [12] and improved and developed in [11], [14]. The composite index of [11] is briefly defined and implemented here as the objective function of the ODGA problem in distribution system.

1) *Energy Loss Index*: This index should be minimized over a considered time horizon. Since each time segment t represents 90-day (30 days per month \times 3 months per season), this index, LI , can be formulated as follows:

$$LI = \frac{EL}{EL^0} \quad (9)$$

where

$$EL = \sum_{s \in \mathcal{S}} \rho_s \sum_{(i,j) \in \mathcal{E}} \sum_{t \in \mathcal{T}} \sum_{h \in \mathcal{H}} r_{ij} \times l_{ij}^s(t, h) \times 90 \quad (10)$$

here, ρ_s is the probability of state s . $EL_{ij}^s(t, h)$ and EL^0 denote the energy-loss after and before DG addition in the system, respectively.

2) *Voltage Profile Index*: This index can be defined as follows:

$$VI = \frac{1}{T \times H} \sum_{s \in \mathcal{S}} \rho_s \sum_{i \in \mathcal{N}} \sum_{t \in \mathcal{T}} \sum_{h \in \mathcal{H}} \gamma_i(t, h) \left(\frac{v_i^s(t, h)}{v_i^0(t, h)} \right) \quad (11)$$

$v_i^0(t, h)$ is the square of the magnitude of complex voltage at bus i at time t at hour h in the base case (without DG). T is the total number of time periods during the planning time horizon and H is the total number of hours in a day. $\gamma_i(t, h)$ is the importance factor of load buses which can be chosen based on the importance and criticality of the loads [11], [14]. For the sake of simplicity, all the load buses are equally weighted in this paper, i.e., $\gamma_i(t, h) = \frac{1}{N}$; $\forall i \in \mathcal{N}$, $\forall t \in \mathcal{T}$, $\forall h \in \mathcal{H}$; here N is the total number of load buses in the system.

It should be noted that the technical indices LI and VI illustrate that employment of DG is beneficial or not. If the introduction of DG is beneficial, LI will be less than unity and VI will be greater than unity.

3) *Multiobjective Index*: The problem of ODGA tries to find minimum energy loss index (9) and/or maximum voltage improvement index (11). When DG is allocated for energy losses minimization, the penetration level may be limited to have maximum voltage profile, and vice versa. To include the effects of the aforementioned indices in the ODGA problem, the following multiobjective index, MOI , can be used as the objective function which should be maximized:

$$MOI = \delta_1 VI - \delta_2 LI \quad (12)$$

here, the weighting factors $0 \leq (\delta_1, \delta_2) \leq 1$, which $\delta_1 + \delta_2 = 1$, indicate relative importance of each index for DGs' allocation. The choice of these factors mainly depends on the experiences and concerns of planners or decision makers. An equal weights are assumed for the proposed indices in this paper.

Generally, the highest value of VI implies DGs allocation is the most beneficial in terms of voltage profile maximization. Also, the lowest value of LI implies the highest benefit in terms of energy losses minimization. Furthermore, the highest MOI implies the maximum benefit of DGs integration in terms of both energy losses reduction and voltage profile improvement.

B. Technical Constraints

1) *Voltage Limits*: The voltage magnitudes should be laid within the pre-specified voltage lower bound, $v_{\min, i}$, and upper bound, $v_{\max, i}$: $\forall i \in \mathcal{N} / \{1\}$, $\forall s \in \mathcal{S}$, $\forall t \in \mathcal{T}$ and $\forall h \in \mathcal{H}$,

$$v_{\min, i} \leq v_i^s(t, h) \leq v_{\max, i} \quad (13)$$

and the voltage magnitude at the root node is as (8).

2) *Feeder Capacity Limits*: Thermal limit of a line is generally assumed stiff and no overloading is permitted. The power flow of each line should be limited to its maximum thermal capacity of line $i \rightarrow j$, $l_{\max, ij}$: $\forall s \in \mathcal{S}$, $\forall t \in \mathcal{T}$ and $\forall h \in \mathcal{H}$,

$$l_{ij}^s(t, h) \leq l_{\max, ij}. \quad (14)$$

3) *Tap Position Constraint of OLTC*: The OLTC model follows standard OPF practice applied in power flow and in the OLTC OPF model [10]. This differs from the model that permits the "best" tap setting to be chosen which have been used in [11]. $\forall t \in \mathcal{T}$ and $\forall h \in \mathcal{H}$,

$$tp_{\min} \leq tp(t, h) \leq tp_{\max}, \quad tp(t, h) \in \text{int} \quad (15)$$

where, tp_{\min} and tp_{\max} are the lower and upper limits on tap position of OLTC. In practice, OLTCs usually possess specified taps; one at center "rated" tap (denoting v_{sub}) and $tp_{\max} = -tp_{\min}$ to increase and decrease the turn ratio. In this paper, $tp \in \{-tp_{\max}, \dots, -1, 0, 1, \dots, tp_{\max}\}$ has been allowed for $\pm 5\%$ variation (each step provides $\alpha = (1.05 - 1)/tp_{\max}$ variation) from the nominal rating of a transformer, v_{sub} , which, in turn, allows for stepwise voltage regulation of the output.

4) *Power Factor Regulation for a DG's Site*: Many DG technologies can operate at a range of power factors. The operating power factor of a DG's site may need to be regulated as considering corresponding standards as follows [11]: $\forall i \in \mathcal{G}, \forall s \in \mathcal{S}, \forall t \in \mathcal{T}$ and $\forall h \in \mathcal{H}$,

$$pf^- \leq \frac{P_{DG,i}^s(t,h)}{\sqrt{P_{DG,i}^s(t,h)^2 + Q_{DG,i}^s(t,h)^2}} \leq 1 \quad (16)$$

where, pf^- is the specified lower limit of the operating power factor of a DG's site.

5) *Maximum Size of DG Units*: Some distribution system companies may have limitations on the percentage of allowed DGs in their systems. So, DG units connected at bus i are constrained to be in a pre-defined discrete sizes:

$$\forall i \in \mathcal{G},$$

$$n_{1,\omega i} \leq n_{1\max,\omega}, \quad n_{1\max,\omega i} \in \text{int}, \quad \forall \omega \in W \quad (17)$$

$$n_{2,x i} \leq n_{2\max,x}, \quad n_{2,x i} \in \text{int}, \quad \forall x \in X \quad (18)$$

$$n_{3,bi} \leq n_{3\max,b}, \quad n_{3,bi} \in \text{int}, \quad \forall b \in B \quad (19)$$

$$P_{W,i} = \sum_{\omega \in W} n_{1,\omega i} \times P_{1,\omega}^r \quad (20)$$

$$P_{pv,i} = \sum_{x \in X} n_{2,x i} \times P_{2,x}^r \quad (21)$$

$$P_{B,i} = \sum_{b \in B} n_{3,bi} \times P_{3,b}^r \quad (22)$$

Equations (17)-(22) show discrete sizes of the wind turbine, PV and biomass DG units, respectively, which can be installed on each bus in the system. $n_{1\max,\omega}$, $n_{2\max,x}$ and $n_{3\max,b}$ are the maximum numbers of WT of type ω , PV module of type x and biomass DG of type b , respectively. $P_{1,\omega}^r$, $P_{2,x}^r$ and $P_{3,b}^r$ are the available nameplate ratings of the wind turbine of type ω , PV of type x and biomass DG of type b , respectively. Aggregation of installed DG capacities at the buses inside the wind zone WP1 and WP2 is given in (23) and (24), respectively:

$$P_{DG,i}^s(t,h) = P_{wp1}^s(t,h) P_{W,i} + P_{pv}^s(t,h) P_{pv,i} + P_{B,i} \quad (23)$$

$$P_{DG,i}^s(t,h) = P_{wp2}^s(t,h) P_{W,i} + P_{pv}^s(t,h) P_{pv,i} + P_{B,i} \quad (24)$$

6) *Maximum DG Penetration Limits*: The sum of installed ratings of DGs on each bus is limited by the maximum allowable penetration on each bus, $P_{bus,i}$: $\forall i \in \mathcal{G}$,

$$P_{W,i} + P_{pv,i} + P_{B,i} \leq P_{bus,i} \quad (25)$$

Overall, the following ODGA problem summarizes the proposed OPF formulation for the radial networks, where the power flows are expressed in the *Distflow* model:

$$\text{ODGA: } \underset{\psi \in \Psi}{\text{maximize}} \quad MOI(\psi) \quad (26)$$

Subject to:

$$(4) - (11), (13) - (25) \quad (27)$$

where, Ψ is the set of decision variables.

V. OMGC IN RDS

The second optimization problem is OMGC. In this problem, the total capacity of ESSs is assumed to be predetermined based on economic studies; therefore, the only goal is to minimize the power exchange between microgrids or power imbalance within the microgrids by proper allocation of reclosers and ESSs. This scenario applies to distribution systems with an existing fuel mix of renewable and dispatchable DG units obtained from previous optimization problem. Two problems are defined here to deal with the problem of the supply-sufficient OMGC in a DG-installed RDS.

A. Problem I: Minimum Power Exchange Between Microgrids

The objective function of this problem is to minimize the annual power exchange between microgrids subject to the power flow equations, ESS constraints and number of protective devices. The protection devices placed on the feeder effectively divide the feeder into so-called microgrids in this paper. In order to minimize the power exchange between microgrids and consider the probabilistic nature of the renewable generations, a new probabilistic index is defined and presented in the objective function. This index represents the probabilistic real and reactive power of the virtual cut set lines (lines including recloser) connecting the microgrids together. The adequacy index below is defined for day t , hour h and $\forall (i,j) \in \mathcal{E}$,

$$SI_{ij}(t,h) = \sum_{s \in \mathcal{S}} \rho_s \cdot (a \times |P_{ij}^s(t,h)| + b \times |Q_{ij}^s(t,h)|). \quad (28)$$

Averaging (28) over the days of the year gives the expected value of $SI_{ij}(t,h)$ for each virtual cut set line, ASI_{ij} , as follows:

$$ASI_{ij} = \frac{1}{T \times H} \sum_{t \in \mathcal{T}} \sum_{h \in \mathcal{H}} SI_{ij}(t,h). \quad (29)$$

The supply security index, SSI , for problem I can be calculated as follows:

$$SSI = \frac{1}{M} \sum_{(i,j) \in \mathcal{R}} \beta_{ij} ASI_{ij} \quad (30)$$

β_{ij} indicates the location of a recloser, that is equal to 1 if line ij is selected to locate a recloser and zero, otherwise. M indicates the number of reclosers to be located in the system which is determined based on the capital investment fund on protective device installation. In a radial feeder, placement of M devices will result in the formation of $M + 1$ microgrids. \mathcal{R} denotes the set of candidate locations of reclosers placement in the system. The following constraint defines that the number of reclosers in the system

$$\sum_{(i,j) \in \mathcal{R}} \beta_{ij} = M. \quad (31)$$

For this optimization problem, in addition to the above mentioned items additional constraints are specified bellow.

1) *Power Flow Equations*: The power flow equations should be modified in order to consider the real power which ESS delivers to (receives from) the grid, $P_{E,i}^s(t, h)$, and reactive power generated by the reactive power compensation equipment such as shunt capacitors and static VAR compensators, $Q_{R,j}^s(t, h)$. In the OPF formulation, the ESS power, $P_{E,i}^s(t, h)$, is positive when the storage is discharging, negative when it is charging, and zero when ESS is in the idle mode.

$$P_{ij}^s(t, h) - r_{ij}l_{ij}^s(t, h) = -p_j^s(t, h) - P_{E,j}^s(t, h) + \sum_{k:j \rightarrow k} P_{jk}^s(t, h) \quad (32)$$

$$Q_{ij}^s(t, h) - x_{ij}l_{ij}^s(t, h) = -q_j^s(t, h) + Q_{R,j}^s(t, h) + \sum_{k:j \rightarrow k} Q_{jk}^s(t, h) \quad (33)$$

2) *ESS Constraints*: The ESS is modeled by (34)-(42). The ESS has three operation modes of charging, discharging and idle [16]. For each ESS $i \in \mathcal{B}$ let $C_i^s(t, h)$, $P_{ch,i}^s(t, h)$ and $P_{dch,i}^s(t, h)$ denote the amount of energy storage, the power input to the ESS and the power output of ESS connected at bus i at day $t \in \mathcal{T}$ at hour $h \in \mathcal{H}$ in scenario $s \in \mathcal{S}$, respectively. The amount of storage for ESS is modeled to follow the first-order difference equation: $\forall i \in \mathcal{B}$, $\forall t \in \mathcal{T}$ and $\forall s \in \mathcal{S}$,

$$C_i^s(t, h) = C_i^s(t, h-1) - \Delta t (P_{dch,i}^s(t, h)/\eta_d - P_{ch,i}^s(t, h)\eta_c) \quad (34)$$

$$P_{E,i}^s(t, h) = P_{dch,i}^s(t, h) - P_{ch,i}^s(t, h) \quad (35)$$

where Δt denotes the time interval $[h-1, h]$. η_d and η_c are the discharge and charge efficiencies of ESS, respectively. The rate of charge/discharge for each ESS connected to bus $i \in \mathcal{B}$, are respectively bounded as follows:

$$0 \leq P_{ch,i}^s(t, h) \leq x_i^s(t, h)P_{ch,i}^{\max} \quad (36)$$

$$0 \leq P_{dch,i}^s(t, h) \leq (1 - x_i^s(t, h))P_{dch,i}^{\max} \quad (37)$$

where binary variable $x_i^s(t, h)$ denotes the charge/discharge state of ESS. If ESS is charging, $x_i^s(t, h) = 1$ and the state of charge will increase. If ESS is discharging, $x_i^s(t, h) = 0$ and the state of charge will decrease. The ESS state of charge at the start and end of each day is obtained by (38) and (39), and limited by (40): $\forall i \in \mathcal{B}$,

$$C_i^s(t, h) = C_i^{\text{end}}, \text{ and } h = H \quad (38)$$

$$C_i^s(t, h) = C_i^0, \text{ and } h = 1. \quad (39)$$

$$0 \leq C_i^s(t, h) \leq C_i^{\max} \quad (40)$$

Finally, total size of ESSs is limited by (41) and (42).

$$\sum_{i \in \mathcal{B}} P_{E,i}^{\max} \leq P^{\max} \quad (41)$$

$$\sum_{i \in \mathcal{B}} C_i^{\max} \leq E^{\max} \quad (42)$$

Hence, the OMGC problem which summarizes the Problem I can be written as bellow:

$$\text{OMGC-P1: } \underset{\varphi \in \Phi}{\text{minimize}} \quad SSI(\varphi) \quad (43)$$

Subject to:

$$(6) - (8), (13) - (16), (32) - (42) \quad (44)$$

where Φ is the set of decision variables.

B. Problem II: Minimum Generation-Load Imbalance in Microgrids

For optimum construction of self-sufficient microgrids, two major points should be considered which are neglected in the problem I: (a) each constructed microgrid includes several interconnected electricity consumers, distributed generators and storage units. As it will be shown in the results, it may be observed a situation in which a constructed microgrid has not any DG or ESS in it which contradicts the definition of the microgrid; (b) in the islanded mode operation, each microgrid should have sufficient power to supply critical loads. These two conditions should be added as important constraints of the optimum microgrid construction problem. For this purpose, the necessary condition for a microgrid to be successful in terms of supply adequacy is that the generation should be greater than or equal to the sum of the critical loads and losses in the islanded mode operation of microgrid m or equivalently:

$$P_D^m + P_{loss}^m - P_G^m \leq 0 \quad (45)$$

where P_G^m and P_D^m are the generated power of DGs plus ESS and load demands connected to the microgrid m , respectively; P_{loss}^m is its power loss which assumed to be 5% of the current load [20]. Since β is a decision variable, the set of nodes belonging to each microgrid m is not specified. For this reason, it is difficult to calculate (45) in a direct procedure. To address this problem, new variables are introduced which are calculated using the forward-backward searches. In this concept, for each $(i, j) \in \mathcal{E}$ forward search gives:

$$d_{ij}^s(t, h) = 1.05\kappa_j P_{D,j}^s(t, h) - P_{G,j}^s(t, h) - P_{E,j}^s(t, h) + \sum_{k:j \rightarrow k} \underbrace{(1 - \beta_{jk})d_{jk}^s(t, h)}_{\psi_{jk}^s(t, h)} \quad (46)$$

and backward search gives: $\forall (i, j) \in \mathcal{E}$,

$$d_{ji}^s(t, h) = 1.05\kappa_i P_{D,i}^s(t, h) - P_{G,i}^s(t, h) - P_{E,i}^s(t, h) + \sum_{\substack{k \in \Omega_i \\ k \neq j}} \underbrace{(1 - \beta_{ik})d_{ik}^s(t, h)}_{\psi_{ik}^s(t, h)} \quad (47)$$

where Ω_i includes the sum of two subsets; the first is the subset of nodes $k \in \mathcal{N}$ so that $(k, i) \in \mathcal{E}$. If node i is connected to greater than two nodes, the subset of nodes $k \in \mathcal{N}$ so that $(i, k) \in \mathcal{E}$ is added to the set Ω_i , too. κ_i is the percentage of sensitive loads connected to the node i . Note that the following constraint should be satisfied $\forall (i, j) \in \mathcal{E}$,

$$\beta_{ij} = \beta_{ji}. \quad (48)$$

Note that, the product of binary variable $(1 - \beta_{ik})$ and bounded continuous variable $d_{ij}^s(t, h) \in [d_{\min}, d_{\max}]$ in equations (46) and (47) is nonlinear. Let \mathcal{E}' denote the collection of all lines. Note that, if $(i, j) \in \mathcal{E}'$ then, $(j, i) \in \mathcal{E}'$. Let $\psi_{ij}^s(t, h)$ denote this product, thus, it can be expressed as the following equivalent linear inequalities: $\forall (i, j) \in \mathcal{E}'$,

$$(1 - \beta_{ij})d_{\min} \leq \psi_{ij}^s(t, h) \leq (1 - \beta_{ij})d_{\max} \quad (49)$$

$$d_{ij}^s(t, h) - \beta_{ij}d_{\max} \leq \psi_{ij}^s(t, h) \leq d_{ij}^s(t, h) - \beta_{ij}d_{\min}. \quad (50)$$

By inspection, it can be observed that if β_{ij} equals one, $\psi_{ij}^s(t, h)$ must vanish due to (49) while the bounds in (50) are inactive. Otherwise, when β_{ij} equals zero, from (50), $\psi_{ij}^s(t, h)$ must be equal to $d_{ij}^s(t, h)$.

Now, to perform the equivalent constraint of (45) while ensuring the mentioned two conditions (a) and (b), the following equation is defined: $\forall (i, j) \in \mathcal{R}$ and for $(i, j) = (1, 2)$,

$$g_{ij}^s(t, h) = d_{ij}^s(t, h) + \psi_{ik}^s(t, h). \quad (51)$$

$g_{ij}^s(t, h)$ represents the left-hand side of (45). The positive values of $g_{ij}^s(t, h)$ denote the amount of insufficient generation or load not served. Equation (52) finds the times and scenarios in which the generation is insufficient in each microgrid. In the case of insufficient generation $\sigma_{ij}^s(t, h)$ would be equal to 1 and zero, otherwise. The equivalent linear formulation of this indicator is as follows:

$$g_{ij}^s(t, h) \leq \sigma_{ij}^s(t, h) \leq 1 + g_{ij}^s(t, h) \quad (52)$$

To explain this, consider the state where there is an insufficient generation, that is $g_{ij}^s(t, h) > 0$. Since $|g_{ij}^s(t, h)| \leq 1$ (as is a per unit value and MVA base value is considered large enough), the lower bound of (52) is strictly greater than zero and less than 1, while the upper bound is greater than 1. Since $\sigma_{ij}^s(t, h)$ is a binary variable, then under insufficient generation, it must be equal to 1. A similar argument applies when there is sufficient generation in which $\sigma_{ij}^s(t, h) = 0$.

The first supply-adequacy metric for the constructed microgrids is defined as follows:

$$IGP_{12} = \frac{1}{T \times H} \sum_{s \in \mathcal{S}} \sum_{t \in \mathcal{T}} \sum_{h \in \mathcal{H}} \rho_s \zeta_{12} \sigma_{12}^s(t, h) \quad (53)$$

$$IGP_{ij} = \frac{1}{T \times H} \sum_{(i,j) \in \mathcal{R}} \beta_{ij} \overbrace{\sum_{s \in \mathcal{S}} \sum_{t \in \mathcal{T}} \sum_{h \in \mathcal{H}} \rho_s \zeta_{ij} \sigma_{ij}^s(t, h)}^{\bar{\sigma}_{ij}} \quad (54)$$

This metric is defined as the product of the probability of the island to be created and the probability of the insufficient generation during microgrid islanded mode. ζ_{ij} is the probability of island to be created for a microgrid connected to node j . An analytical model based on segmentation concept can be implemented to calculate this probability for each microgrid [20]. Using this curtailment indicator, the probability of curtailment scenarios over all constructed microgrids, IGP , can be calculated. In this paper, it is assumed that the second node always falls into the first constructed microgrid (see (53)), and other microgrids take into account by implementing β_{ij} in the equation (54). It should be noted that, (54) is nonlinear because of the product of binary variable β_{ij} and continuous variable $\bar{\sigma}_{ij} \in [y_{\min}, y_{\max}]$. Let π_{ij} denote this product, now it can be linearized using the following equivalent linear inequalities: $\forall (i, j) \in \mathcal{R}$,

$$\beta_{ij}y_{\min} \leq \pi_{ij} \leq \beta_{ij}y_{\max} \quad (55)$$

$$\bar{\sigma}_{ij} - (1 - \beta_{ij})y_{\max} \leq \pi_{ij} \leq \bar{\sigma}_{ij} - (1 - \beta_{ij})y_{\min}. \quad (56)$$

It can be observed that if β_{ij} equals zero, π_{ij} must vanish due to (55) while the bounds in (56) are inactive. Otherwise, when β_{ij} equals one, from (56), π_{ij} must be equal to $\bar{\sigma}_{ij}$. Hence, by substituting π_{ij} in (54), average value of IGP over constructed microgrids can be calculated as the following linearized form:

$$IGP = \frac{1}{M+1} \left(IGP_{12} + \sum_{(i,j) \in \mathcal{R}} IGP_{ij} \right). \quad (57)$$

IGP can not measure the amount of insufficient generation in each constructed microgrid, thus, the expected insufficient generation, EIG , is introduced as another supply-adequacy metric as follows:

$$EIG = \sum_{s \in \mathcal{S}} \rho_s \sum_{t \in \mathcal{T}} \sum_{h \in \mathcal{H}} \zeta_{ij} \sigma_{12}^s(t, h) g_{12}^s(t, h) \times 90 + \sum_{(i,j) \in \mathcal{R}} \beta_{ij} \sum_{s \in \mathcal{S}} \sum_{t \in \mathcal{T}} \sum_{h \in \mathcal{H}} \rho_s \zeta_{ij} \sigma_{ij}^s(t, h) g_{ij}^s(t, h) \times 90. \quad (58)$$

This metric is nonlinear due to the product of binary variables β_{ij} and $\sigma_{ij}^s(t, h)$, and continuous variable $g_{ij}^s(t, h) \in [g_{\min}, g_{\max}]$. Let $\xi_{ij}^s(t, h) = \sigma_{ij}^s(t, h) g_{ij}^s(t, h)$ which can be linearized using the same procedure in (55) and (56). Now, suppose that

$$\bar{g}_{i,j} = \sum_{s \in \mathcal{S}} \sum_{t \in \mathcal{T}} \sum_{h \in \mathcal{H}} \rho_s \zeta_{ij} \xi_{ij}^s(t, h) \times 90 \quad (59)$$

and let $\varphi_{ij} = \beta_{ij} \bar{g}_{i,j}$ and $\phi_{12}^s(t, h) = \sigma_{12}^s(t, h) g_{12}^s(t, h)$. These nonlinear products can be also linearized with the same manner in (55) and (56). Therefore, the linearized form of (58) can be written as follows:

$$EIG = \sum_{s \in \mathcal{S}} \rho_s \sum_{t \in \mathcal{T}} \sum_{h \in \mathcal{H}} \zeta_{12} \phi_{12}^s(t, h) \times 90 + \sum_{(i,j) \in \mathcal{R}} \varphi_{ij}. \quad (60)$$

To adequately measure the degree of supply-adequacy for the constructed microgrids throughout a year, the proposed probabilistic-based indices, i.e., IGP and EIG should be minimized. The following MILP-based OMGC problem summarizes the Problem II:

$$\text{OMGC-P2:} \quad \underset{\gamma \in \Gamma}{\text{minimize}} \quad IGP(\gamma) \quad (61)$$

Subject to:

$$(46) - (52), (55), (56) \quad (62)$$

where Γ is the set of decision variables.

VI. NUMERICAL SIMULATION

A. Test System Data

The proposed problem of the optimal placement and smart operation of WGs has been applied to the IEEE 33-bus radial test distribution system. This system has a peak demand of 3.715 MW and 2.300 MVar [26]. While in annual energy terms, the aggregated demand profile implies an annual consumption of 610 MWh and 406 MVarh. Base values of this system are 12.66 kV and 100 MVA. The substation voltage magnitude is assumed at nominal value in the base

TABLE I
CANDIDATE BUSES FOR DG INTEGRATION

DG type	Candidate buses
Wind	3,6,9,12,15,18,21,24,27,30,33
PV	2,4,8,10,14,16,20,22,26,28,32
Biomass	5,7,11,13,17,19,23,25,29,31

TABLE II
OPTIMUM LOCATION(SIZE-KW) OF DG'S OBTAINED BY ODGA PROBLEM

DG type	Passive operation	Active operation
Wind	12(50),15(100),30(100),33(100)	12(50),15(100),30(100),33(100)
PV	10(25),14(50),16(50),32(50)	10(25),14(50),16(50),32(50)
Biomass	13(150),17(125),29(75),31(200)	7(25),13(125),17(125),29(75), 31(200)

case (no DG). The constraint of operating voltages is assumed $\pm 5\%$ of nominal value. The OLTC target voltage is assumed to be 1.05. Detailed load and branch data of this test system can be obtained from [26]. The maximum thermal limits of lines are set to 6.6 MVA (which corresponds to a current of 300 A). The hourly wind speed and solar irradiance data for the site under study have been utilized to generate a Rayleigh and Beta PDFs for each time segment, respectively. From the hourly load data for the system under study and the IEEE-RTS system [25], the load profile is assumed as a percentage of the annual peak load.

The obtained MINLP optimization models (i.e., ODGA and OMGC-P1) and MILP optimization model (i.e., OMGC-P2) were coded in the GAMS optimization modeling environment [27] and solved using DICOPT and CPLEX solvers, respectively on a computer with Pentium(R) Dual-Core CPU @ 2 GHz and 4 GB of RAM.

B. Optimal DG Allocation: passive vs active operation of network

With the consideration of the capital investment fund and land space limits on DG installation, the total rated capacity installation limits of DGs (with discrete size of 25 kW) at each candidate bus are assumed to be 100 kW, 50 kW and 200 kW, respectively for wind turbine, PV and biomass DG units. Potential sites for the installation of DG units are given in Table I.

For the obtained probabilistic model of generation and load demand, and for a given candidate location of DGs, the proposed stochastic OPF problems are performed over a horizon of one year for the passive operation of system and two smart grid control schemes. It can be seen that the active management of the network improves its performance in terms of energy losses and voltage profile. This is primarily due to the ability of the coordinated voltage control (CVC) scheme to alleviate voltage rise problems. Also, the PFC strategy allows DGs to inject reactive power during peak periods and absorb reactive power during off peak periods. Optimal size and location of DGs are recorded for these operation scenarios, see Table II. As can be seen, the adoption of smart grid control strategies compared to the passive operation, allows a further energy loss reduction and voltage profile improvement by optimally integrating biomass DG capacities in the more locations of the system. Table III presents the optimum values of MOI , LI , VI and minimum voltage magnitude, i.e., $\min V$, under various operation strategies

TABLE III
ODGA IN PASSIVE AND ACTIVE OPERATION CONDITIONS

Index	Passive operation	Active operation
MOI	0.19	0.23
LI	0.60	0.56
VI	1.02	1.06
$\min V$	0.97	0.99

TABLE IV
LOCATIONS OF PROTECTION DEVICES AND RELATED ISLAND CREATION PROBABILITIES

Line	5-6	6-26	7-8	11-12	15-16	16-17	17-18	29-30
ζ_{ij}	0.023	0.025	0.024	0.076	0.088	0.090	0.110	0.073

without exceeding voltage or thermal limits. Take a brief look, it can be observed that MOI in the active operation of network will be greater than its value when passive operation is adopted. The value of multiobjective index, MOI , is 0.19 under the passive operation of system whereas, incorporating smart grid control strategies will increase this value by more than 21%. However, as can be observed from Table III, compared to the base case (without DG), considerable benefits are achieved by optimally allocation of DGs in the system. Assuming passive management of the network, unity power factor operation of the DG units sees energy losses reduced by 40% from the original (no DG) configuration. If smart grid control schemes are incorporated, then energy losses are cut by more than 44%.

C. Optimal Microgrid Construction in Distribution System

The previously designed system is considered as the base system for distribution system partitioning. In this step, optimum microgrid construction is performed to optimally select the location of reclosers and ESS sizing in the system. The validity of the proposed method is demonstrated by comparing with the method recently reported in [8]. For this purpose, the base system is partitioned into the self-sufficient microgrids without and with considering ESSs. The formulation of this reference was extended and developed in this paper to solve the problem of optimum microgrid construction considering SSI as the objective function. On the other hand, the proposed optimization problem, i.e., OMGC-P2, uses the objective of minimizing insufficient generation probability of the constructed microgrids, i.e., IGP . The proposed adequacy-based metrics are used to compare the results of OMGC problem.

Candidate locations of protection devices and related island creation probabilities, ζ_{ij} , are given in Table IV. Also, ζ_{12} is assumed equal to 0.02 and the percent of critical loads in each load bus, κ_i , is assumed to be 50%. Tables V and VI show the results and optimum locations of the reclosers to construct the supply-sufficient microgrids (with M equal to 4) by utilizing the optimization problems OMGC-P1 and OMGC-P2, respectively. The results of these problems are given in Table V, Table VI, Table VIII, Fig. 4 and Fig. 5. As one would expect, index SSI is not a good objective function for OMGC problem. Therefore, OMGC-P1 cannot guarantee the above-mentioned conditions (a) and (b) because node 18 (i.e., microgrid m4) is selected as the virtual microgrid with no DGs connected to it (see Table V and Fig. 4). It can be observed that constructed microgrid m4 is the most unreliable microgrid with

TABLE V
OPTIMUM CONSTRUCTED MICROGRIDS BY OMGC-P1 WITHOUT ESS

Constructed microgrid	Nodes in each microgrid	IGP	EIG (MWh)
m1	1 to 10,19 to 21,23 to 25,26 to 29	0.02	108.8
m2	12 to 15	0.00	0.000
m3	16,17	0.00	0.000
m4	18	0.11	190.8
m5	30 to 33	0.002	0.038
Average		0.0264	60

TABLE VI
OPTIMUM CONSTRUCTED MICROGRIDS BY OMGC-P2 WITHOUT ESS

Constructed microgrid	Nodes in each microgrid	IGP	EIG (MWh)
m1	1 to 5,19 to 21,23 to 25	0.02	87.07
m2	6 to 16	0.023	37.65
m3	17,18	0.00	0.000
m4	26 to 29	0.00	0.000
m5	30 to 33	0.002	0.038
Average		0.009	24.95

and without EES with a *IGP* of 0.11 and *EIG* of 190.8 MWh. In overall, the constructed microgrids using OMGC-P1 are more unreliable than that of OMGC-P2 with *IGP* of 0.0264 and *EIG* of 60 MWh. It can be seen from Table VI that the proposed OMGC-P2 problem is reduced these metrics to 0.009 and 25 MWh, respectively.

In the next step we optimally allocate reclosers and ESS using both OMGC-P1 and OMGC-P2 to construct optimum self-sufficient microgrids. The aggregated energy capacity and power rating of all ESSs on all buses are set as 400 kW and 3.5 MWh, respectively. It is assumed that the battery efficiency is 100%, i.e., $\eta_d = \eta_{ch} = 1$. The candidate locations for allocation of ESSs are assumed in set $\mathcal{B} = \{10, 12, 14, 16, 32\}$.

The results of the optimal placement of reclosers as well as ESSs allocation in the 33-bus RDS are shown in Fig. 4, Fig. 5, Table VII and Table VIII. ESSs are introduced to the system to reduce the negative impact of the intermittent renewable energy resources. It can be seen that the OMGC-P1 has a limited ability in the optimal partitioning of the system by implementing ESSs. The results show no change in the location of reclosers in this problem with respect to before adding ESSs. By using this model, with and without ESS consideration, no improvement can be seen on the supply adequacy of the constructed microgrids. On the contrary, by considering EESSs, OMGC-P2 can improve the adequacy of constructed microgrids by reducing the value of *IGP* by 50%. The reason is that, in comparison to the OMGC-P1, OMGC-P2 permits more ESSs capacity to be installed (i.e., 131 kW greater capacity). Thus, the number of states representing insufficient generation are reduced.

VII. CONCLUSION

In this paper, a new methodology is proposed for optimal construction of microgrids by optimally allocating DGs, ESSs and reclosers in RDS. Firstly, a probabilistic OPF technique is developed and utilized for optimal allocation of wind-based, PV and biomass DG units in the smart distribution systems to maximize the multiobjective performance index by properly assign and aggregate energy

TABLE VII
OPTIMAL RESULTS OF CONSTRUCTED MICROGRIDS WITH ESSs OBTAINED BY OMGC-P1 AND OMGC-P2

constructed microgrid	OMGC-P1		OMGC-P2	
	IGP	EIG	IGP	EIG
m1	0.02	108.8	0.02	118.02
m2	0.00	0.000	0.003	7.401
m3	0.00	0.000	0.00	0.000
m4	0.11	187.4	0.00	0.000
m5	0.00	0.000	0.00	0.000
Average	0.0264	59.24	0.0046	25.084

TABLE VIII
OPTIMUM SIZE (LOCATION) OF ESS BY DIFFERENT OPTIMIZATION MODELS

Model	P_E^{\max} (kW) (node)
OMGC-P1	47(12),23(14),53(16),100(32)
OMGC-P2	90(10),100(12),100(14),21(16),43(32)

losses reduction and voltage improvement impact indices in it. The optimization problem has demonstrated that adopting smart grid-based control schemes such as CVC and PFC can harvest significant benefits in terms of loss reduction and voltage improvement. Next, the obtained DG-enhanced system is clustered into microgrids by optimally placement of reclosers and ESSs in the system for maximizing supply adequacy of the constructed microgrids. To solve this problem, two different optimization problems have been developed. New metrics to evaluate supply-adequacy of microgrids are developed and formulated in linear forms in OMGC-P2 problem.

The results demonstrate the effectiveness of the proposed optimization problem OMGC-P2 for optimal partitioning of smart distribution systems into self-sufficient microgrids. Finally, it is noted that the proposed mathematical formulation is generic, accordingly, the objective function can be expanded to augment additional terms such as reliability, economic and environmental concerns of DGs, ESSs and reclosers allocations for optimal construction of microgrids. The future works of this study is to investigate the robustness of optimal results under the future load growth and taking into account the uncertainty of probabilistic DG penetration on distribution systems in the construction of optimum microgrids.

REFERENCES

- [1] G. Boyle, *Renewable energy*. OXFORD university press, 2004.
- [2] H. L. Willis, *Distributed power generation: planning and evaluation*. CRC Press, 2000.
- [3] T. Niknam, M. Zare, and J. Aghaei, "Scenario-based multiobjective volt/var control in distribution networks including renewable energy sources," *IEEE Trans. Power Del.*, vol. 27, no. 4, pp. 2004–2019, Oct. 2012.
- [4] "Impact of increased penetration of photovoltaic generation on power systems," *IEEE Guide for Design, Operation, and Integration of Distributed Resource Island Systems With Electric Power Systems*, Jul. 20 2011, IEEE Std 1547.4-2011.
- [5] Y. Seyedi, H. Karimi, and S. Grijalva, "Distributed generation monitoring for hierarchical control applications in smart microgrids," *IEEE Trans. Power Syst.*, vol. 32, pp. 2305–2314, May 2017.
- [6] T. Niknam, "An efficient algorithm for volt/var control at distribution systems including der," *J. Intell. Fuzzy Syst.*, vol. 20, pp. 119–132, Aug. 2009.
- [7] S. A. Arefifar, Y. A.-R. I. Mohamed, and T. H. M. EL-Fouly, "Optimum microgrid design for enhancing reliability and supply-security," *IEEE Trans. Smart Grid*, vol. 4, no. 3, pp. 1567–1575, Sep. 2013.
- [8] S. A. Arefifar, Y. A.-R. I. Mohamed, and T. H. M. EL-Fouly, "Supply-adequacy-based optimal construction of microgrids in smart distribution systems," *IEEE Trans. Smart Grid*, vol. 3, no. 3, pp. 1491–1502, Sep. 2012.

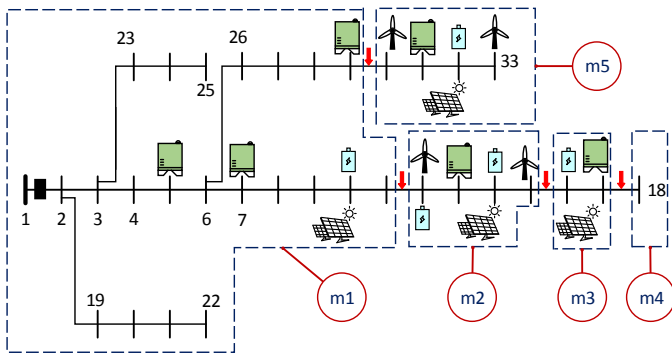


Fig. 4. Optimal constructed microgrids with ESS obtained by OMGC-P1

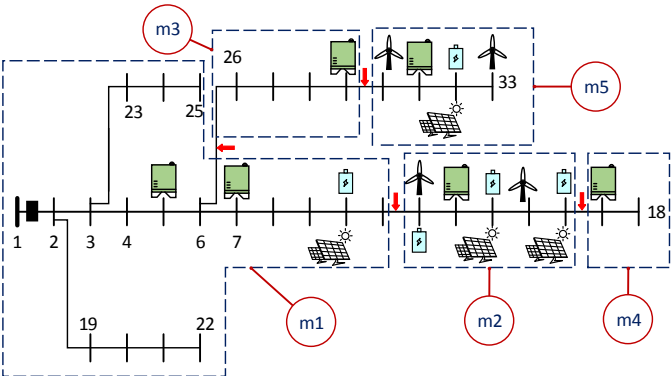


Fig. 5. Optimal constructed microgrids with ESS obtained by OMGC-P2

- [9] M. H. Moradi, M. Abedini, and S. M. Hosseinian, "A combination of evolutionary algorithm and game theory for optimal location and operation of DG from DG owner standpoints," *IEEE Trans. Smart Grid*, vol. 7, no. 2, pp. 608–616, Mar. 2016.
- [10] S. Wang, S. Chen, L. Ge, and L. Wu, "Distributed generation hosting capacity evaluation for distribution systems considering the robust optimal operation of OLTC and SVC," *IEEE Trans. Sustain. Energy*, vol. 7, no. 3, pp. 1111–1123, Jul. 2016.
- [11] M.-A. Akbari, J. Aghaei, and M. Barani, "Convex probabilistic allocation of wind generation in smart distribution networks," *IET Renew. Power Gener.*, May 2017.
- [12] P. Chiradeja and R. Ramakumar, "An approach to quantify the technical benefits of distributed generation," *IEEE Trans. Energy Convers.*, vol. 19, no. 4, pp. 764–773, Dec. 2004.
- [13] R. Shayani and M. de Oliveira, "Photovoltaic generation penetration limits in radial distribution systems," *IEEE Trans. Power Syst.*, vol. 26, no. 3, pp. 1625–1631, Aug. 2011.
- [14] M. A. Akbari, J. Aghaei, M. Barani, M. Savaghebi, M. Shafie-khah, J. M. Guerrero, and J. P. S. Catalao, "New metrics for evaluating technical benefits and risks of DGs increasing penetration," *IEEE Trans. Smart Grid*, vol. PP, no. 9, pp. 1–1, 2017.
- [15] S. Wang, Z. Li, L. Wu, M. Shahidepour, and Z. Li, "New metrics for assessing the reliability and economics of microgrids in distribution system," *IEEE Trans. Power Syst.*, vol. 28, no. 3, pp. 2852–2861, Aug. 2013.
- [16] S. Bahramirad, W. Reder, and A. Khodaei, "Reliability-constrained optimal sizing of energy storage system in a microgrid," *IEEE Trans. Smart Grid*, vol. 3, no. 4, pp. 2056–2062, 2012.
- [17] A. Kavousi-Fard, M. A. Rostami, and T. Niknam, "Reliability-oriented reconfiguration of vehicle-to-grid networks," *IEEE Trans. Ind. Informat.*, vol. 11, pp. 682–691, June 2015.
- [18] R. Karki and R. Billinton, "Reliability/cost implications of pv and wind energy utilization in small isolated power systems," *IEEE Trans. Energy Convers.*, vol. 16, no. 4, pp. 368–373, 2001.
- [19] A. Pregelj, M. Begovic, and A. Rohatgi, "Recloser allocation for improved reliability of DG-enhanced distribution networks," *IEEE Trans. on Power Syst.*, vol. 21, pp. 1442–1449, Aug 2006.
- [20] Y. M. Atwa, E. F. El-Saadany, M. M. A. Salama, R. Seethapathy, M. Assam, and S. Conti, "Adequacy evaluation of distribution system including wind/solar

DG during different modes of operation," *IEEE Trans. on Power Syst.*, vol. 26, pp. 1945–1952, Nov 2011.

- [21] A. Safdarian, M. Fotuhi-Firuzabad, and F. Aminifar, "Compromising wind and solar energies from the power system adequacy viewpoint," *IEEE Trans. Power Syst.*, vol. 27, pp. 2368–2376, Nov 2012.
- [22] Z. Salameh, B. Borowy, and A. Amin, "Photovoltaic module-site matching based on the capacity factors," *IEEE Trans. Energy Convers.*, vol. 10, no. 2, pp. 326–332, Jun. 1995.
- [23] N. Amjady, J. Aghaei, and H. A. Shayanfar, "Stochastic multiobjective market clearing of joint energy and reserves auctions ensuring power system security," *IEEE Trans. Power Syst.*, vol. 24, no. 4, pp. 1841–1854, Nov. 2009.
- [24] N. Growe-Kuska, H. Heitsch, and W. Romisch, "Scenario reduction and scenario tree construction for power management problems," in *Power Tech Conference Proceedings*, vol. 3, IEEE, 2003.
- [25] J. M. S. Pinheiro, C. R. R. Dornellas, M. T. Schilling, A. C. G. Melo, and J. C. O. Mello, "Probing the new IEEE reliability test system (RTS-96): HL-II assessment," *IEEE Trans. Power Syst.*, vol. 13, pp. 171–176, Feb 1998.
- [26] M. E. Baran and F. F. Wu, "Network reconfiguration in distribution systems for loss reduction and load balancing," *IEEE Trans. Power Del.*, vol. 4, pp. 1401–1407, Apr. Apr. 1989.
- [27] B. A. McCarl, A. Meeraus, P. van der Eijk, M. Bussieck, S. Dirkse, P. Steacy, and F. Nelissen, "Mccarl gams user guide," 2014. [Available online]:<http://www.gams.com>.